

## Nanopore-based technologies beyond DNA sequencing

Ying, Yi Lun; Hu, Zheng Li; Zhang, Shengli; Qing, Yujia; Fragasso, Alessio; Maglia, Giovanni; Meller, Amit; Bayley, Hagan; Dekker, Cees; Long, Yi Tao

**DOI**

[10.1038/s41565-022-01193-2](https://doi.org/10.1038/s41565-022-01193-2)

**Publication date**

2022

**Document Version**

Final published version

**Published in**

Nature Nanotechnology

**Citation (APA)**

Ying, Y. L., Hu, Z. L., Zhang, S., Qing, Y., Fragasso, A., Maglia, G., Meller, A., Bayley, H., Dekker, C., & Long, Y. T. (2022). Nanopore-based technologies beyond DNA sequencing. *Nature Nanotechnology*, 17(11), 1136-1146. <https://doi.org/10.1038/s41565-022-01193-2>

**Important note**

To cite this publication, please use the final published version (if applicable).  
Please check the document version above.

**Copyright**

Other than for strictly personal use, it is not permitted to download, forward or distribute the text or part of it, without the consent of the author(s) and/or copyright holder(s), unless the work is under an open content license such as Creative Commons.

**Takedown policy**

Please contact us and provide details if you believe this document breaches copyrights.  
We will remove access to the work immediately and investigate your claim.

***Green Open Access added to TU Delft Institutional Repository***

***'You share, we take care!' - Taverne project***

**<https://www.openaccess.nl/en/you-share-we-take-care>**

Otherwise as indicated in the copyright section: the publisher is the copyright holder of this work and the author uses the Dutch legislation to make this work public.



# Nanopore-based technologies beyond DNA sequencing

Yi-Lun Ying<sup>1,6</sup>, Zheng-Li Hu<sup>1,6</sup>, Shengli Zhang<sup>2,6</sup>, Yujia Qing<sup>3,6</sup>, Alessio Fragasso<sup>4,6</sup>, Giovanni Maglia<sup>1,2</sup>, Amit Meller<sup>5</sup>, Hagan Bayley<sup>3</sup>, Cees Dekker<sup>4</sup> and Yi-Tao Long<sup>1</sup>

**Inspired by the biological processes of molecular recognition and transportation across membranes, nanopore techniques have evolved in recent decades as ultrasensitive analytical tools for individual molecules. In particular, nanopore-based single-molecule DNA/RNA sequencing has advanced genomic and transcriptomic research due to the portability, lower costs and long reads of these methods. Nanopore applications, however, extend far beyond nucleic acid sequencing. In this Review, we present an overview of the broad applications of nanopores in molecular sensing and sequencing, chemical catalysis and biophysical characterization. We highlight the prospects of applying nanopores for single-protein analysis and sequencing, single-molecule covalent chemistry, clinical sensing applications for single-molecule liquid biopsy, and the use of synthetic biomimetic nanopores as experimental models for natural systems. We suggest that nanopore technologies will continue to be explored to address a number of scientific challenges as control over pore design improves.**

Nanopores as single-molecule biosensors were initially developed for ultrasensitive DNA sequencing and other label-free biomolecular sensing techniques<sup>1–5</sup>. They register geometrically confined single molecules that bind within or translocate through their interior volumes to allow label-free sensing<sup>6</sup>. In a typical nanopore measurement, individual analytes enter the nanopore under an applied potential, which alters the flow of ions through the nanopore and is reflected in a time-dependent current recording. By analysing the modulation of the ionic current in terms of the blockade amplitude, duration and frequency, nanopores have been applied to the stochastic sensing and characterization of DNA<sup>7–10</sup>, RNA<sup>11</sup>, peptides<sup>12,13</sup>, proteins<sup>14,15</sup>, metabolites and protein–DNA complexes<sup>16</sup> at the single-molecule level. In particular, the success of nanopore-based DNA/RNA sequencing has stimulated many potential applications in a relatively simple, high-throughput and label-free format.

Ideally, the nanopore dimensions should be comparable to those of the analyte for the presence of the analyte to produce a measurable change in the ionic current amplitude above the noise level. Nanopores can be formed in several ways, with a wide range of pore diameters. Biological nanopores are formed by the self-assembly of either protein subunits, peptides or even DNA scaffolds in lipid bilayers or block copolymer membranes<sup>1,3,6,17,18</sup>. They possess atomically precise dimensions controlled by biopolymer sequences, providing the ability to recognize biomolecules with constriction diameters of ~1–10 nm. Solid-state nanopores are crafted in thin inorganic or plastic membranes (for example, SiN<sub>x</sub>), which allows the nanopores to have extended diameters of up to hundreds of nanometres, permitting the entry or analysis of large biomolecules and complexes. The tools for fabricating solid-state nanopores, which include electron/ion milling<sup>4,5</sup>, laser-based optical etching<sup>19,20</sup> and the dielectric breakdown of ultrathin solid membranes<sup>21,22</sup>, can be used to manipulate nanopore size at the nanometre scale, but

allow only limited control over the surface structure at the atomic level in contrast to biological nanopores. The chemical modification and genetic engineering of biological nanopores, or the introduction of biomolecules to functionalize solid-state nanopores<sup>23</sup>, can further enhance the interactions between a nanopore and analytes, improving the overall sensitivity and selectivity of the device<sup>2,17,24–26</sup>. This feature allows nanopores to controllably capture, identify and transport a wide variety of molecules and ions from bulk solution.

Nanopore technology was initially developed for the practicable stochastic sensing of ions and small molecules<sup>2,27,28</sup>. Subsequently, many developmental efforts were focused on DNA sequencing<sup>1,7–9</sup>. Now, however, nanopore applications extend well beyond sequencing, as the methodology has been adapted to analyse molecular heterogeneities and stochastic processes in many different biochemical systems (Fig. 1). First, a key advantage of nanopores lies in their ability to successively capture many single molecules one after the other at a relatively high rate, which allows nanopores to explore large populations of molecules at the single-molecule level in reasonable timeframes. Second, nanopores essentially convert the structural and chemical properties of the analytes into a measurable ionic current signal, even achieving enantiomer discrimination<sup>29</sup>. The technology can be used to report on multiple molecular features while circumventing the need for labelling chemistries, which may complicate the overall analysis process and affect the molecular structures. For example, nanopores can discriminate nearly 13 different amino acids in a label-free manner, including some with minute structural differences<sup>30</sup>. An important aspect is the ability of nanopores to identify species<sup>31</sup> that lack suitable labels for signal amplification or whose information is hidden in the noise of analytical devices. Consequently, nanopores may serve well in molecular diagnostic applications required for precision medicine, which achieves the identification of nucleic acid, protein or metabolite analytes and other biomarkers<sup>11,32–35</sup>.

<sup>1</sup>State Key Laboratory of Analytical Chemistry for Life Science, School of Chemistry and Chemical Engineering, Nanjing University, Nanjing, People's Republic of China. <sup>2</sup>Groningen Biomolecular Sciences and Biotechnology Institute, University of Groningen, Groningen, the Netherlands. <sup>3</sup>Department of Chemistry, University of Oxford, Oxford, UK. <sup>4</sup>Department of Bionanoscience, Kavli Institute of Nanoscience, Delft University of Technology, Delft, the Netherlands. <sup>5</sup>Faculty of Biomedical Engineering, Technion-IIT, Haifa, Israel. <sup>6</sup>These authors contributed equally: Yi-Lun Ying, Zheng-Li Hu, Shengli Zhang, Yujia Qing, Alessio Fragasso. ✉e-mail: [giovanni.maglia@rug.nl](mailto:giovanni.maglia@rug.nl); [ameller@technion.ac.il](mailto:ameller@technion.ac.il); [hagan.bayley@chem.ox.ac.uk](mailto:hagan.bayley@chem.ox.ac.uk); [C.Dekker@tudelft.nl](mailto:C.Dekker@tudelft.nl); [yitaolong@nju.edu.cn](mailto:yitaolong@nju.edu.cn)

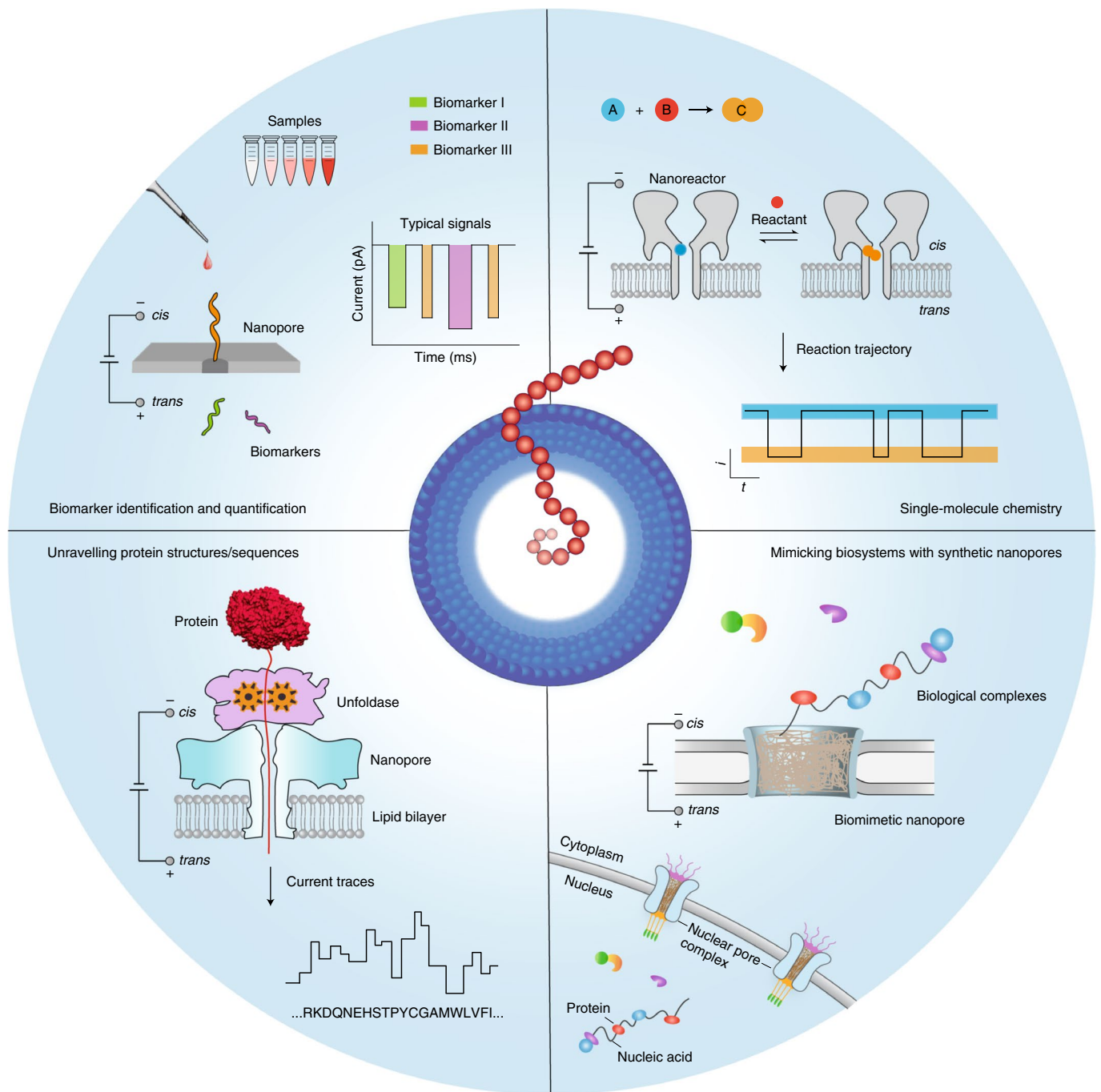


**Fig. 1 | Nanopore technologies beyond DNA sequencing.** Four areas of research in which nanopores have great potential to contribute to new knowledge and new technologies are shown. The protein structure is from <https://www.rcsb.org/structure/6DCW>.

Third, nanopores provide a well-defined scaffold for controllably designing and constructing biomimetic systems, which involve a complex network of biomolecular interactions. These nanopore systems track the binding dynamics of transported biomolecules as they interact with nanopore surfaces, hence serving as a platform for unravelling complex biological processes (for example, the transport properties of nuclear pore complexes)<sup>36–39</sup>. Fourth, chemical groups can be spatially aligned within a protein nanopore, providing a confined chemical environment for site-selective or regioselective covalent chemistry. This strategy has been used to engineer protein nanoreactors to monitor bond-breaking and bond-making events<sup>40,41</sup>.

Here we discuss the latest advances in nanopore technologies beyond DNA sequencing and the future trajectory of the field, as well as the opportunities and main challenges for the next decade. We specifically address the emerging nanopore methods for protein analysis and protein sequencing, single-molecule covalent chemistry, single-molecule analysis of clinical samples and insights into the use of biomimetic pores for analysing complex biological processes.

### Characterization of single proteins with nanopores

Academic efforts are now shifting towards studying proteins after the spectacular success of nucleic acid sequencing using nanopore technology. As organisms such as ourselves support millions of

different proteins, the challenges in proteomics involve identifying the proteins, quantifying their abundance and characterizing the choreography of the post-translational modifications that underlie their function. Several approaches to protein identification are being explored.

Folded proteins have been sensed using solid-state<sup>42,43</sup> and biological<sup>44–46</sup> nanopores. Properties such as protein volume, dipole and shape can be inferred by analysing the translocation dynamics of proteins through solid-state nanopores<sup>47,48</sup>, indicating that nanopores are useful for extracting the generic properties of proteins. Alternatively, ligands such as biotin<sup>14</sup>, aptamers<sup>45,49</sup>, protein domains<sup>50</sup> or antibodies<sup>51,52</sup> can directly attach to biological nanopores even in the presence of complex media, such as serum (Fig. 2a). Moreover, proteins can be identified using DNA carriers modified with protein-specific binders as they translocate into nanopores<sup>53,54</sup>. Beyond characterizing single proteins, nanopore arrays or specific fractionation protocols will most probably be required to address the complexity of proteomes.

Work is underway to use biological nanopores to detect single peptides or proteins as an alternative to mass spectrometry, the workhorse of proteomic analysis. Following initial work with model peptides<sup>12,13,55,56</sup> and post-translational protein modifications<sup>57</sup>, it has been reported that, as observed previously for polyethylene glycol (PEG) molecules<sup>58</sup>, peptide signals are related to their volume<sup>59,60</sup> (and hence to a first approximation to the peptide molecular weight). Although the interactions between peptides and nanopores are likely to play an important role for a given class of nanopore<sup>26</sup>, other important properties of peptide, such as hydrophobicity, charge or folds, should be revealed instead. Another considerable step in this field of research was the realization that by lowering the pH to less than 4, most peptides can be nearly uniformly charged and captured irrespective of their chemical composition<sup>61</sup>, although an electro-osmotic flow was manipulated to capture peptides with a different net charge at near-physiological pH<sup>62</sup>. Based on peptide volume recognition, a single-molecule protein identifier has been proposed in which a protease is placed directly above a biological nanopore, and the fragmented peptides are sequentially read by a nanopore sensor (Fig. 2b)<sup>63</sup>. Initial steps to integrate a peptidase with a protein nanopore have been made<sup>63</sup>.

However, the ideal approach to nanopore proteomics would be *de novo* protein sequencing, where proteins are unfolded, linearly translocated across a nanopore amino acid by amino acid, and individual amino acids are recognized by specific current signatures. Using biological nanopores, several laboratories have observed the differences in single amino acids in either peptides<sup>61,64,65</sup> or stretched polypeptides<sup>57,66</sup>. Therefore, at least a subset of amino acids or post-translational modifications should be addressable by nanopore current measurements. Attempts have also been made to control the translocation of linearized proteins using unfoldases—enzymes that unfold proteins using adenosine 5'-triphosphate as fuel<sup>67,68</sup>. In a proof-of-concept example, controlled transport was facilitated by the ClpXP unfoldase–protease pair, which was used to pull on proteins prethreaded through an  $\alpha$ -haemolysin nanopore. The narrow entry of the nanopore was then used as a sieve to forcefully unfold the proteins (Fig. 2c)<sup>68</sup>. Differences in proteins or modifications that affect the folded state of the protein have been reported. Another approach used a proteolytically inactivated proteasome—a cylindrical multicatalytic system that degrades proteins—genetically fused atop a  $\beta$ -barrel protein nanopore<sup>63</sup>. The proteasome acted as a docking station for an unfoldase, which would then feed unfolded protein to the proteasome chamber and eventually through the nanopore. Both approaches require further developments, either to reduce the electrical signal generated by the unfolding process at the mouth of the nanopore<sup>68</sup> or to control the stretching of the proteins as they translocate through the nanopore<sup>63</sup>. Recent works seem to have led to a breakthrough in peptide sequencing. Thus, it has been

reported that a DNA helicase was used to ratchet a DNA–peptide hybrid molecule through a nanopore, and single amino acid substitutions from negatively charged peptides were detected in individual peptides<sup>69–71</sup>.

In addition to identifying proteins, nanopores can be used as single-molecule sensors to characterize protein activity, dynamics and conformational changes. Among the unique advantages of nanopores is their ability to sample native proteins at the single-molecule level with microsecond resolution and no intrinsic limitation on the observation period. In the first implementations of nanopore enzymology, biological nanopores were used to monitor the formation of the products of bulk enzymatic reactions<sup>72,73</sup>, which might be useful when a straightforward spectroscopic assay is not available. However, this approach does not allow the activities of individual enzymes to be determined. The latter was first achieved by following the enzymatic ratcheting of a DNA strand across a nanopore in real time<sup>9,74</sup>, a method developed for DNA sequencing applications. For example, these studies revealed that Hel308 helicase moves a distance corresponding to half a DNA base during nucleotide binding and half a base during nucleotide hydrolysis, and that the motor proteins of Phi29 DNA polymerase and Hel308 occasionally backstep while incorporating nucleobases or moving along DNA. Another approach has been used to monitor enzyme binding to the nanopore itself. Previous studies observed conformational changes in GroEL binding to a GroES nanopore<sup>75</sup>, or kinases binding or phosphorylating a peptide that is introduced within the transmembrane region of a nanopore<sup>76</sup>. However, the relatively complex engineering of nanopores is likely to limit this approach to bespoke examples.

A more generic approach is to temporarily trap a protein inside a biological nanopore. Conformational changes or dynamics can then be obtained through changes in the nanopore signal (Fig. 2d). Proteins of 20–65 kDa can be captured by electro-osmotic flow within asymmetric biological nanopores with relatively large diameters of >3 nm, such as engineered cytolysin A (ClyA)<sup>45</sup> or two-component pleurotolysin (PlyAB)<sup>46</sup>, for variable periods. Notably, at moderate voltages (<150 mV), no evidence of protein unfolding was observed<sup>77</sup>. Ligand-induced conformational changes for a range of proteins<sup>78–80</sup> have been reported using biological nanopores. These include the tiny conformational changes of dihydrofolate reductase (DHFR) during ligand binding<sup>80</sup> and catalysis<sup>81</sup>, which could not be observed previously by single-molecule fluorescence resonance energy transfer experiments. The results of these studies revealed that DHFR exists in multiple fixed conformations—conformers—whose exchange during catalysis is probably used to tune enzyme efficiency<sup>80,81</sup>.

Solid-state nanopores have also been used to sample protein conformations<sup>82</sup>. However, the fast transport across nanopores often prevents multiple exchanges within single enzymes. This limitation has been addressed recently. In one example, a protein stopper was introduced to immobilize a biotinylated peptide inside a nanopore, allowing the measurement of multiple conformational transition pathways (Fig. 2e)<sup>83</sup>. In another recent report, a DNA lid was added to one side of a lipid-coated nanopore, and proteins were added to the opposite side (Fig. 2f)<sup>84</sup>. The electrophoretic force allowed the DNA origami sphere to cover the nanopore, and the induced electro-osmotic flow was used to trap a range of different proteins on the opposite side. Multiple conformational transitions of the individual chaperone Hsp90 protein could be observed using this so-called nanopore electro-osmotic trap (NEOtrap).

### Single-molecule chemistry within biological nanopores

Single-molecule sensing generally involves non-covalent interactions<sup>3</sup>. Advances in this area suggest that covalent chemistry may be examined in a similar manner, and indeed the bond-making and bond-breaking events of individual molecules attached to the



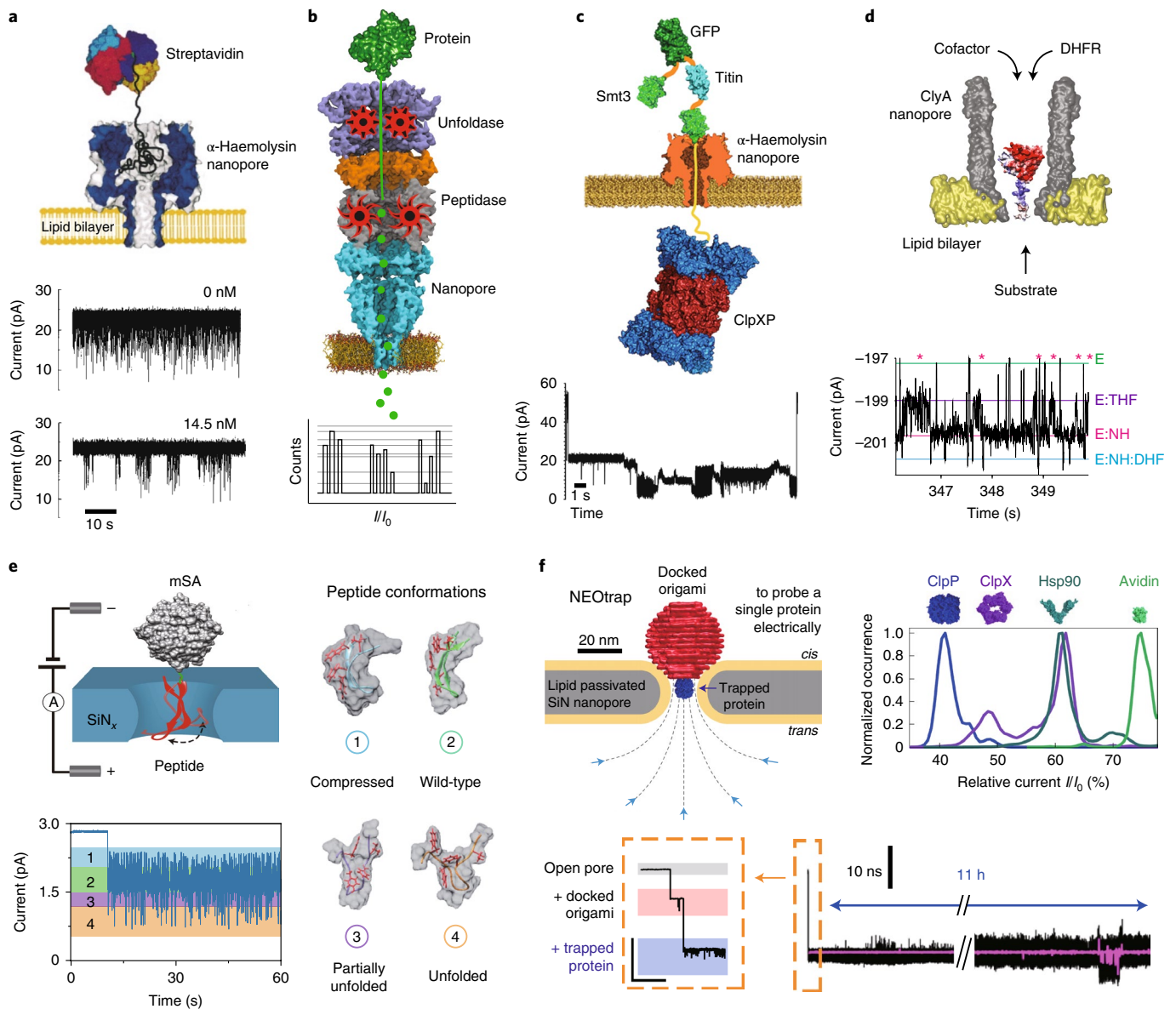


**Fig. 2 | Unravelling proteins with nanopores.** **a**, Identification of the concentration of a mutant streptavidin by an  $\alpha$ -haemolysin nanopore covalently modified with PEG-biotin (top), as observed by a reduction in the current noise during binding events (bottom)<sup>14</sup>. The increase of mutant streptavidin concentration led to decrease in frequencies of the blockade events. **b**, Schematic of a single-molecule identifier in which a protein (for example, superfolder green fluorescent protein, GFP; dark green) is fed to an unfoldase (purple) and a peptidase (coloured in orange and grey) attached to a nanopore (cyan)<sup>63</sup>. An illustration of the peptide fragmentation pattern is shown below. The transport of the proteolytic peptides produced different current variations, leading to distinct residual current ( $I$ ) from the open pore current ( $I_0$ ), where  $I/I_0$  represents the relative residual current blockade. **c**, Co-translational unfolding transport of a construct that includes Smt3 (light green), GFP (dark green) and titin (cyan), previously electrophoretically captured using a peptide thread (yellow), through a nanopore operated by ClpXP (coloured in blue and red) (top). The unfolded translocation is shown as the electrical signal (bottom)<sup>68</sup>. **d**, Catalytic activity of DHFR (coloured according to vacuum electrostatics using PyMOL) inside a ClyA nanopore (grey, top), as shown by representative traces (bottom). Product formation is indicated by pink asterisks<sup>81</sup>, which involve the complexes of the enzyme DHFR (E) with NADPH (E:NH), tetrahydrofolate (E:THF) and then dihydrofolate (E:NH:DHf). **e**, Dynamic conformation of a single peptide confined in a SiN<sub>x</sub> solid-state nanopore (top left). The  $\beta$ -hairpin peptide is bound to monovalent streptavidin (mSA). The ionic current (bottom left) reflects different conformations of the target peptide for unravelling the folding/unfolding pathway (right)<sup>83</sup>. **f**, Immobilization of a protein (blue) inside a nanopore (grey) using a DNA origami sphere (red) as a NEOtrap (top left)<sup>84</sup>. The current trace indicates a trapping time of several hours, and the inset displays the trapping process of a single protein, from an open pore (grey band) to DNA origami docking (red band) and protein trapping (blue band) (bottom). The relative current histograms reveal distinguishable distributions of ClpP, ClpX, Hsp90 and avidin proteins of different masses, sizes and shapes trapped by origami docking (top right). Panels adapted with permission from: **a**, ref. 14, Springer Nature Ltd; **b**, ref. 63, Springer Nature Ltd; **c**, ref. 68, American Chemical Society; **d**, ref. 81, American Chemical Society; **e**, ref. 83, RSC; **f**, ref. 84, Springer Nature Ltd.

interior wall of a nanopore can be analysed on the basis of their modulation of the ionic current<sup>40</sup>. Biological nanopores engineered to contain reactive sites are referred to as protein nanoreactors.

Examples include many aspects of the chemistry of thiols introduced as cysteine side chains<sup>85</sup>. Groups other than thiols can be examined after they have been introduced by site-directed chemical

modification<sup>86</sup> or as non-canonical amino acids incorporated by native chemical ligation<sup>87</sup>. The nanoreactor approach has been used to examine various aspects of photochemistry<sup>88</sup>, unravel the stereochemical course of transformations<sup>85</sup>, observe polymerization step by step<sup>89</sup> and monitor a primary isotope effect<sup>90</sup>. Catalytic cycles have been reconstituted by sampling partial reaction sequences in a nanopore after extricating intermediates from solution<sup>91</sup>, and reaction networks of considerable complexity that would be hard to deconvolute by NMR spectroscopy have been disentangled<sup>185</sup>.

The strengths and weaknesses of the nanoreactor approach with regard to single-molecule covalent chemistry must be considered. On the plus side, no tagging of reactants is required. As the pores formed by bacterial proteins are generally highly stable, a wide range of pH values, salt concentrations and temperatures<sup>92</sup> can be used. However, so far, only aqueous chemistry has been examined. Both irreversible and reversible chemistry have been explored, and because there are two compartments in a bilayer set-up, incompatible spatially separated reactants can be used<sup>93</sup>. Attachment to the wall of the lumen is required to prevent diffusion out of a pore during a reaction sequence and to prevent kinetic complications, such as the dimerization of intermediates<sup>87</sup>. If repeated turnover at a defined site is considered to be catalysis, examples have been observed<sup>93</sup>, but further progress in the use of nanopores to alter the course and rate of reactions is expected. Computer analysis of the frequency and lifetime of current states produces reaction schemes and kinetic constants for covalent chemistry with time resolutions that can reach the 100- $\mu$ s range<sup>94</sup>. In general, the standard deviations of rate constants are more than  $\pm 5\%$ , which can be limiting—for example, only large isotope effects can be detected<sup>90</sup>. While the nanoreactor approach provides a single-molecule reaction trajectory in which all steps are visible whether or not they are rate-limiting, the molecular identification of intermediates can be problematic, as in any single-molecule approach.

In early work, the kinetics of covalent chemistry within a nanoreactor were assumed to approximate the kinetics of ensemble reactions in bulk solution, and this is roughly correct for small molecules<sup>40</sup>. More recently, interest has turned to considerations of how the environment within a nanopore, notably confinement, neighbouring groups and chirality, can affect chemistry, especially that of polymers, and how electrophoresis and electro-osmosis<sup>95</sup> can drive reactants into and out of pores. To enable the chemical manipulation of a polymer, its translocation through a nanoreactor can be arrested by either a terminal protein stopper or covalent linkage to the internal wall (Fig. 3a). In the presence of a pulling force imposed by either electrophoresis or electro-osmosis, the polymer will extend and elongate within the tubular structure. Additional force is exerted as the polymer emerges from confinement and regains conformational entropy. Two features of nanopore confinement are advantageous for chemical manipulation. First, reactive groups spatially separated along the polymer chain can be aligned with inward-facing reactive side chains. Second, the direction of the pulling force on a covalently attached polymer, and thereby the polymer's orientation, can be switched by reversing the applied potential, resetting the chemical landscape.

Alignment within a nanoreactor has been exploited to effect selective chemistry under confinement<sup>96</sup>. As a proof of concept, the interchange between disulfides in polymer backbones and cysteine thiols at different positions within a nanopore was examined (Fig. 3b). The turnover of polymer substrates was enabled by using a competing small-molecule reductant (1,4-dithiothreitol). Site selectivity was assessed as the fraction of a particular polymer that reacted at a particular location within a nanoreactor. The regioselectivity between two chemically equivalent sulfur atoms in a disulfide was determined by observing the characteristic currents associated with each reaction product. Both site selectivity and regioselectivity showed strong dependence on the locations of the cyste-

ines in the nanopore and the disulfides in the polymer. This strategy might be adapted to other synthetic tubular nanosystems, such as metal–organic frameworks, to facilitate site-selective or regioselective chemistry.

The selective chemistry promoted by confinement has been further developed into a processive molecular machine<sup>97</sup>, a ‘hopper’ that moves along a cysteine track within a nanopore while carrying a DNA cargo (Fig. 3c)<sup>98</sup>. The hopper takes subnanometre steps through consecutive thiol–disulfide interchange reactions. Reactions producing backwards motion are strongly disfavoured when there is a pulling force on the DNA, endowing the hopper with remarkable directionality. External control of the applied potential reorients the DNA within the nanopore and thereby resets the direction of hopping and the endpoint of the process. Hopping is highly processive<sup>98</sup> and may provide a chemical alternative to the enzymatic ratchets used in sequencing technologies, if longer tracks can be provided, for example, on a patterned surface<sup>99</sup>. Furthermore, this process could be applied to polypeptides and polysaccharides, as well as nucleic acids.

### Synthetic nanopores for mimicking biological systems

While nanopores understandably attract the most attention for their use in sequencing and bioanalytical applications, they also offer exciting opportunities to study questions that arise in cell biology. Cells feature a wide variety of nanometre-sized pores within their membranes (Fig. 4a) that act as gateways for molecular transport between compartments. For example, the flow of ions and small molecules (such as adenosine 5'-triphosphate) is regulated by ion channels and transporters, with crucial roles in homeostasis, energy production, cellular communication and sensory transduction<sup>100</sup>. Larger pores, such as the mitochondrial translocase<sup>101</sup> and the nuclear pore complex (NPC)<sup>102</sup>, are responsible for regulating the transport of proteins and RNAs between cellular compartments. However, other examples include the SecYEG protein secretion pore<sup>103</sup>, the ClpXP protease<sup>104</sup> used for protein degradation, the ceramide pores involved in cellular apoptosis<sup>105</sup>, pore-forming toxins such as  $\alpha$ -haemolysin<sup>106</sup> and the viral motor protein for the packaging of DNA<sup>107</sup>. Biomolecular transport across all these pores poses many mechanistic questions, which often can be studied by extracting pores from the cell and docking them within a planar lipid membrane for the *in vitro* characterization of their transport properties. However, the high complexity of the pores, such as NPCs, prevent such a reconstitution approach.

With recent advances in solid-state nanopores<sup>23</sup>, protein nanopore engineering<sup>6,40</sup> and DNA nanotechnology<sup>108</sup>, it is now possible to build artificial systems that recapitulate the functionality of biological pores *in vitro*. There are many examples of engineered nanopore-based systems that can act as minimal mimics, including asymmetric solid-state nanopores for the realization of ion pumps<sup>109</sup>, and ion-gated<sup>110</sup> and pH-gated<sup>111</sup> pores that mimic switchable ion channels. Other notable biomimetic nanopore systems include synthetic DNA origami pores for the reconstitution of synthetic ligand-gated ion channels<sup>38</sup> or highly efficient lipid scramblases<sup>112</sup>, while biological nanopores have been designed to mimic passive<sup>113</sup> or active<sup>114</sup> membrane transporters<sup>115</sup>. Beyond reproducing the behaviour of biological channels, such biomimetic pores have great potential for enhancing our understanding of complex biological processes that cannot be probed directly *in vivo*.

A notable example is the NPC, a large ( $\sim 52$  MDa in yeast<sup>116</sup>) multiprotein complex that forms large pores ( $\sim 40$  nm) within the nuclear envelope to regulate all molecular traffic in and out of the nucleus (Fig. 4b). Although much is known about its biological function<sup>117</sup>, a solid understanding of its transport properties is lacking. In fact, the astounding complexity of the *in vivo* environment, combined with the fact that the central channel of the NPC is composed of intrinsically disordered proteins, prevents the elucidation of a full mecha-

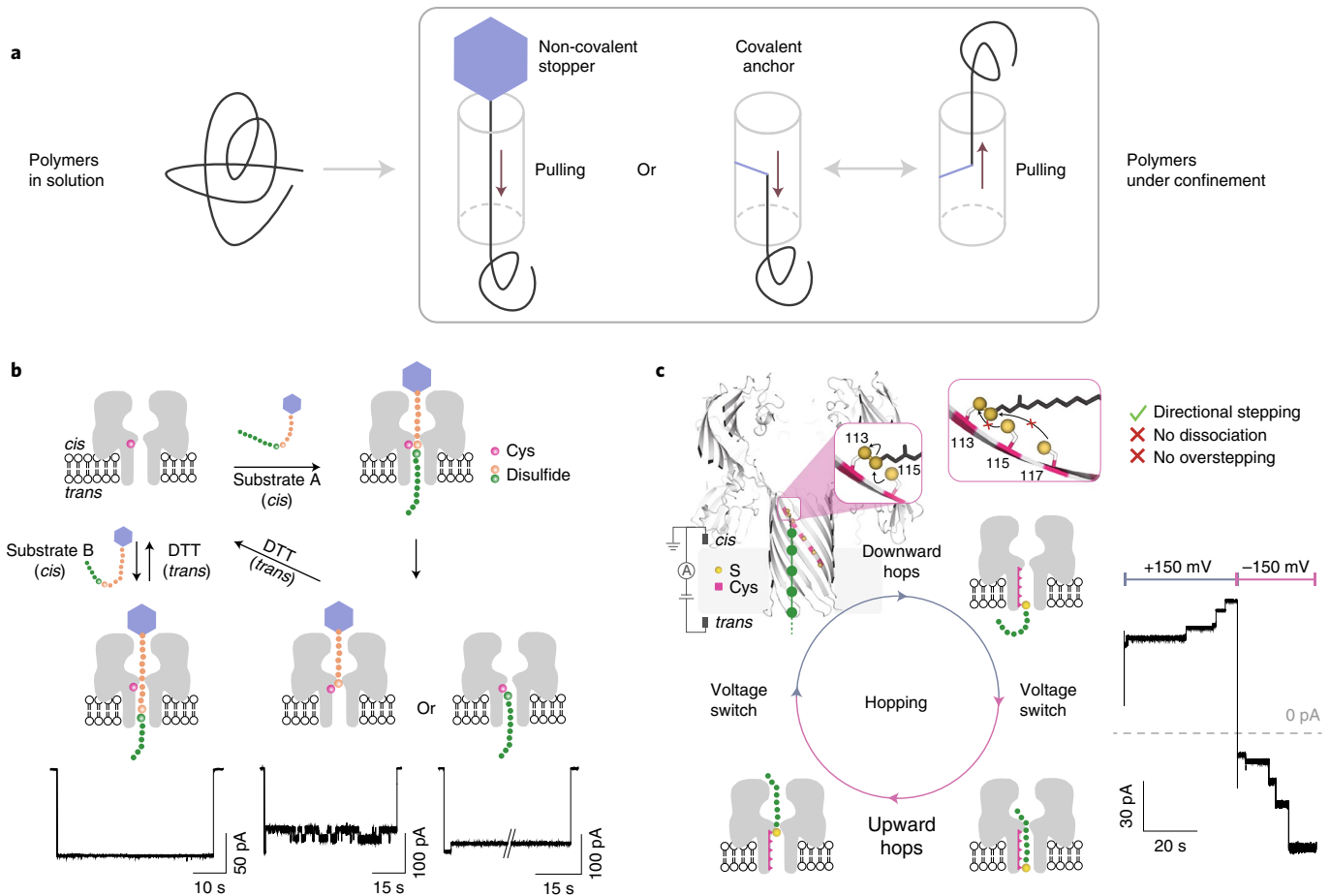


**Fig. 3 | Chemistry of polymers under confinement.** **a**, Polymers, which coil in solution, are extended when confined within a tubular protein nanoreactor. This is achieved by non-covalently or covalently anchoring one end of the polymer and applying a pulling force, for example, an applied electric potential. With covalent linkages, the polymer can be extended in either direction. **b**, Extending a polymer within a tubular nanoreactor exposes its reactive site (for example, a disulfide) to a reactive group positioned on the nanoreactor interior (for example, a cysteine thiol)<sup>96</sup>. In this way, spatial alignment differentiates between chemically equivalent reactive sites (top). Site selectivity and regioselectivity are determined at the single-molecule level by ionic current recording (bottom). The turnover of polymer substrates is enabled by 1,4-dithiothreitol (DTT). **c**, A molecular hopper moves along a multi-cysteine track under an applied potential while carrying a DNA cargo (green circles)<sup>98</sup>. Ratcheted by selective thiol-disulfide interchange reactions, the hopper makes steps in the direction of the pulling force (left). Real-time tracking of the hopper on the track is achieved by monitoring the ionic current (right). Reversal of the applied potential flips the hopper, which then moves in the opposite direction. Panels adapted with permission from: **b**, ref. <sup>96</sup>, Springer Nature Ltd; **c**, ref. <sup>98</sup>, AAAS.

nistic picture of nuclear transport. The NPC conduit is filled with a 'spaghetti-like' mesh of intrinsically disordered proteins, called FG nucleoporins (FG-Nups), rich in F and G amino acid repeats, which are the key elements of gatekeeper function. While small molecules can freely pass, larger cargo (>40 kDa proteins or messenger RNA) is blocked unless it is bound to nuclear transport receptors, which can actively partition into the FG-Nup mesh. The basis for such selectivity is still debated, and many open questions remain, for example, with regard to the spatial arrangement of FG-Nups and whether nuclear transport receptors partake in establishing a selective barrier beyond being mere transporters of cargo. The NPC is a prime example of a system where biomimetic nanopores could help to disentangle these major mechanistic questions.

Biomimetic NPCs have been developed in the past decade. The 30-nm pore arrays functionalized with purified FG-Nups can behave selectively<sup>36</sup>; that is, they allow nuclear transport receptors to efficiently pass but block other proteins. This showed for the first time that the FG-Nup mesh alone is sufficient to impart a selective transport barrier, which is a striking finding considering that the biomimetic NPCs consisted of only one type of FG-Nups, whereas

native NPCs feature more than ten different types of FG-Nups. Selective transport across individual biomimetic nanopores could be measured by grafting FG-Nups to the inner walls of a solid-state nanopore (Fig. 4c), with ionic current measurements providing single-molecule resolution<sup>37</sup>. These biomimetic NPCs provided the first insights into the conformation of FG-Nups within the pore by examining the behaviour of the conductance as a function of pore diameter. Follow-up work emphasized the key role of the hydrophobic residues of the FG-Nups, as the corresponding mutants whose hydrophobic amino acids were replaced by hydrophilic amino acids lost their selectivity altogether<sup>118</sup>. These experiments, coupled with molecular dynamics simulations, revealed the important role of the cohesiveness of the FG-Nup mesh for achieving proper selective behaviour. More recently, nanopores functionalized with user-defined protein sequences that mimicked native FG-Nups were also shown to be selective, demonstrating the outstanding robustness of FG-Nups towards drastic changes in their amino acid sequence<sup>39</sup>. A creative, alternative approach to mimicking NPCs is the use of a DNA origami ring as a scaffold with programmable sites for anchoring FG-Nups (Fig. 4d)<sup>17,18,119</sup>. This platform was used to



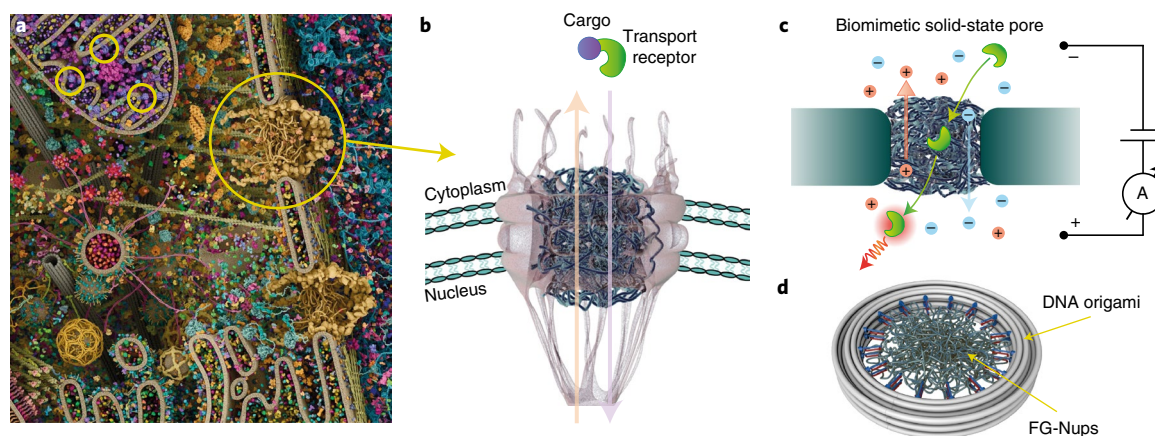


**Fig. 4 | Biomimetic NPCs based on nanopores.** **a**, Sketch of the interior of a eukaryotic cell. The yellow circles indicate an NPC (right) and three mitochondrial pores (left). **b**, Schematic of the NPC. The dark blue filaments represent the FG-Nup mesh. The NPC spans the nuclear membrane, which comprises two lipid bilayers. Import (purple) and export (orange) transport pathways are indicated. **c**, Schematic of a biomimetic solid-state nanopore, with FG-Nups (dark blue) grafted onto the solid-state nanopore, allowing the transport of biomolecules to be measured electrically or optically. **d**, Sketch of a biomimetic NPC built by attaching FG-Nups (dark blue) to a DNA origami scaffold (grey). Credit: **a**, Gael McGill (<https://gaelmcgill.artstation.com/projects/Pm0JL1>); **b**, Adapted with permission from S. S. Patel (Royal Thimphu College).

image the spatial arrangements of confined FG-Nups using cryo-electron microscopy and atomic force microscopy, and allows the exploration of more complex FG-Nup meshes that combine different types of FG-Nups.

#### Biomarker identification and quantification using nanopores

The adaptation of nanopore sensing technologies in clinical methodology presents new challenges associated with the greater complexity and heterogeneous nature of medical specimens compared with laboratory-made samples (Fig. 5). Additionally, clinical sensing also requires extremely high precision, specificity and sensitivity, which further complicates its implementation. Nevertheless, the potential ability of nanopores to offer a generic and highly flexible sensing platform for bodily fluids (liquid biopsy) stands out as a high-impact opportunity that has begun to be addressed only in recent years.

Two primary factors can be identified as the main roadblocks in realizing this vision. First, unlike laboratory-made ‘analytical samples’, the target biomolecules in clinical samples (often nucleic acids or protein biomarkers) span a large range of concentrations, from as low as tens of attomolar ( $10^{-18}$  M) for some blood pathogenic infections and circulating tumour DNAs to subnanomolar ( $10^{-9}$  M) for severe acute respiratory syndrome (SARS), influenza and other biomarkers<sup>120</sup>. In many cases, super-low biomarker concentrations severely limit the use of standard purification/concentration techniques<sup>121</sup>. Second, most clinical samples contain an abundance of constituents that may interfere with the nanopore sensor itself (that is, blocking the nanopore or causing false translocation events). In particular, bodily fluids such as plasma, urine and nasal secretions can clog the nanopore prematurely. Moreover, bulk purification assays, including liquid chromatography and ‘clean-up’ columns, which are widely used in life sciences research, are not optimal for nanopore-based single-molecule sensing as they are lossy, time-consuming and may not transfer well to point-of-care applications.

In recent years, researchers have begun to tackle these challenges by developing smart assays and devices for the treatment of clinical samples, taking advantage of some of the unique capabilities of nanopore sensors. In particular, owing to their extremely small and compact form factor, nanopore sensors can be integrated into microfluidic devices used for either sample preparation or

analyte concentration, further increasing the yield of detection<sup>122</sup>. Moreover, biophysical concentration strategies, for example, those that involve dielectrophoretic trapping or isotachopheresis focusing, can in principle concentrate the target species by several orders of magnitude and therefore have potential for the future development of liquid biopsy applications involving biomolecule-based disease prognostics and diagnostics<sup>123</sup>.

A number of biochemical assays have already been developed to enhance molecular specificity and circumvent the negative effects of background molecules on nanopore functionality. These assays involve minimal losses of target molecules during sample preparation while at the same time protecting the nanopore by the selective degradation of background molecules. For example, a biological nanopore-based direct, digital counting of single-nucleotide polymorphic sites marked with locked nucleic acid–synthetic molecules was used for the detection of Shiga toxin-producing *Escherichia coli* serotype and cancer-derived driver mutations<sup>35,124</sup>. Another approach using solid-state nanopores capitalized on the extremely high specificity of DNA ligase to pull down selected circulating tumour DNA mutations associated with breast cancer genes (that is, *ERBB2* and *PIK3Ca*) in blood samples<sup>34</sup>. These mutations were sensed optically by tagging the probe oligonucleotides with fluorescent dyes and supplementing the electrical sensing of the nanopore with a single-molecule optical detection approach. Solid-state nanopores were also used to quantify global 5-hydroxymethylcytosine epigenetic DNA modifications in human tissue derived from both healthy breast tissue and stage 1 breast tumour tissue<sup>125</sup>. In another recent study, the high selectivity of DNA aptamers was used to fabricate specific DNA ‘carriers’ with high affinities for specific protein biomarkers in a plasma sample, producing characteristic electric current traces when translocated through a nanopore formed at the end of a glass-pulled pipette<sup>126</sup>. Similarly, the unique nanopore electrical signatures of DNA–peptide nucleic acid–peptide complexes targeting anti-human immunodeficiency virus, tumour-necrosis factor- $\alpha$  or tetanus toxin were used to quantify low levels of the antibodies extracted from saliva swabs<sup>127</sup>. Taking advantage of electro-optical sensing, short hairpin-structured oligonucleotides containing fluorophore and quencher moieties (‘molecular beacons’) were used to mark and identify specific complementary DNA molecules from human serum and urine as they were forced through the tip of a nanopipette<sup>128</sup>.

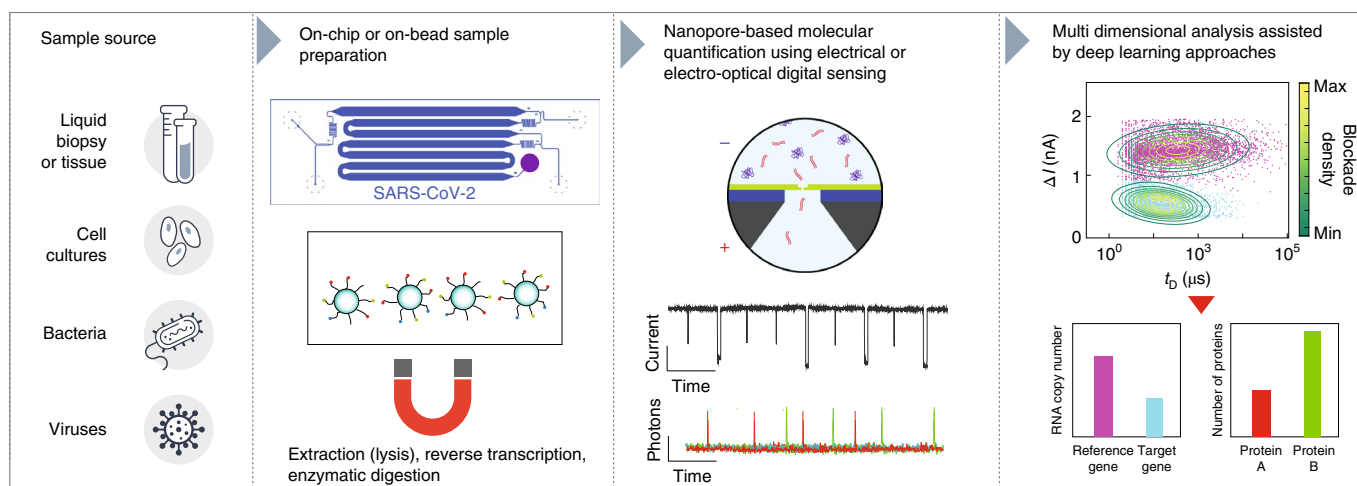


**Fig. 5 | Adapting nanopore sensing for biological samples and clinical diagnostics.** A variety of biomedical sample sources, including bodily fluids, tissue biopsies or biological specimens such as cell cultures, bacteria and viruses, can be collected through minimal and non-lossy biochemical treatment for single-molecule sensing with biological or solid-state nanopores. The ultrasmall sample volume (for example, a microlitre or less) required for the analysis lends itself to hands-free assay development using on-chip microfluidics and/or magnetic beads. Nanopore sensing may involve either the pure, electrical digital counting of biomolecules or combined electro-optical sensing to enhance the multiplexing ability of the system. Data analysis is supported by advanced machine-learning approaches for classifying and counting the target biomolecules.  $t_b$  is the duration of target blockade in nanopore sensing.

An alternative strategy for sensing protein biomarkers in biofluids has been explored involving the creation of a protein bait antibody connected to a biological nanopore, hence serving as a local ‘trap’ for the target protein<sup>52,129</sup>. Specifically, outer membrane protein G with a short, biotinylated polymer chain was used as a sensing probe. The binding/unbinding kinetics of several anti-biotin antibodies (including monoclonal antibodies) were studied in a buffered solution of diluted serum. Interestingly, the different anti-biotin antibodies showed remarkably different binding/unbinding kinetics, presumably due to different antibody sizes, shapes or charges. A similar approach involved a truncated t-FhuA protein pore equipped with a short hexapeptide tether, a barnase protein receptor and a dodecapeptide adapter<sup>50</sup>. The capture and release events of a protein analyte by the tethered protein bait occurred outside the nanopore and were accompanied by uniform current opening, whereas non-specific pore penetrations by non-target components of the serum incurred irregular current blockades. As a result of this unique peculiarity of the readout between specific protein captures and non-specific pore penetration events, which result in highly dynamic ion current signatures, this selective sensor can quantitatively sample proteins and has the potential to provide richer information on detected analytes than classical immunosorbent assays.

The  $\alpha$ -haemolysin protein pore was used to selectively detect microRNA (miR) molecules hybridized in solution to oligonucleotide probes, allowing the quantification of the miR-155 biomarker from the purified plasma samples of lung cancer patients<sup>32</sup>. The specific binding of the miR to the probe molecules generated long, voltage-driven unzipping events that were readily sensed by analysing the ion current traces<sup>130</sup>. More recently, a purification-free method for the nanopore-based digital counting of mRNA expression was demonstrated<sup>121</sup>. The method involves the reverse transcription of the target genes, directly followed by the enzymatic degradation of the background molecules with no intermediate purification stages. The accuracy of the assay relies on designing highly specific reverse transcription primers and avoiding polymerase chain reaction (PCR) amplification, which could lead to erroneous amplification in cases where the clinical sample contains small amounts of the target mRNA biomarker. The method was

used to quantify mRNA cancer biomarkers, such as MACC1, as well as for the PCR-free sensing of SARS coronavirus 2 (SARS-CoV-2) clinical samples, potentially showing greater accuracy than the gold-standard quantitative PCR with reverse transcription method.

Nanopore sensing of clinical samples is not limited to nucleic acids and proteins. Recently, it was found that the method used to measure the conformational changes in proteins lodged inside a biological nanopore could also be adapted to sense the concentration of metabolites, such as glucose and asparagine<sup>33</sup> or vitamin B1 (ref. <sup>131</sup>), directly from bodily fluids (blood, sweat, urine and saliva). Hundreds of substrate-binding proteins exist in nature that recognize their cognate ligands through large conformational changes, which could then be used to recognize a wide variety of metabolites. Other examples include the indirect detection of thyroid-stimulating hormone from human serum samples using a magnetic bead-based sandwich assay<sup>132</sup> and the sensing of drugs, such as cocaine, in human serum or saliva by means of an aptamer-ssDNA complex, which undergoes strand displacement and translocation through a nanopore in the presence of the drug<sup>133</sup>. Additionally, hyaluronic acid, which plays a critical role in tissue hydration, inflammation and joint lubrication, was quantified in synovial fluid using solid-state nanopores. The hyaluronic acid molecules were isolated using hyaluronan-binding protein-coated magnetic beads before the target molecules were released for nanopore sensing<sup>134</sup>.

In all the examples provided for the nanopore-based sensing of clinical biomarkers, the ability to sense multiple species (for example, DNAs, RNAs and metabolites) using the same nanopore is a direct consequence of the single-molecule nature of the technique in which only one molecule is sensed at a time, and a dynamic ion current trajectory over time is used as the basis for target multiplexing. This illustrates the great potential that nanopore sensing holds for future complex biofluid characterization, often involving a multitude of biomarkers.

### Conclusion and perspectives

This Review has outlined diverse nanopore research directions and applications beyond DNA sequencing. Tremendous progress has been made over the past two decades. Nanopores have become an essential single-molecule tool in multiple disciplines, including

chemistry, biophysics and nanoscience. However, there are still challenges to overcome before the full potential of nanopore technology can be attained. For example, improvements in sensing accuracy and temporal resolution will be necessary to uncover the exact chemical compositions of single biopolymers (for example, proteins or polysaccharides). Specifically, proteins consist of 20 natural amino acids and polysaccharides of more than 10 monosaccharide units compared with just the 4 nucleobases in DNA. Therefore, nanopores will most probably require tailoring, as the volume of the sensing region should be of comparable size to a single unit of the biopolymer. More importantly, the nanopore should be optimally sensitive to the chemical or physical properties of the building blocks, producing distinguishable ionic current signatures for each unit. This could be achieved by carefully functionalizing a pore's inner surfaces to manipulate the interactions between the biopolymer and the nanopore, providing the required sensitivity, selectivity and capture efficiency. Interesting directions to explore are the *de novo* design of nanopores<sup>135,136</sup> and the synthesis of DNA origami scaffolds<sup>137,138</sup>, which will allow the size and shape of nanopores to be tailored beyond the abilities of current engineering methods. The use of non-natural amino acids<sup>87</sup> may expand the diverse chemical functionalities of biological nanopores to facilitate the study of covalent and non-covalent reactions under nanopore confinement. While the functionalization of solid-state nanopores with natural elements has proven fruitful, the incorporation of new modalities, such as optically, magnetically and electrochemically sensitive chemical groups (for example, porphyrin derivatives and radical polymers) and materials (for example, MXenes and nanocrystals), at the pore interface is worth exploring to allow spectrometric readouts (for example, Raman scattering and fluorescence) and facilitate the active control of the detection process (such as feedback between interaction and analysis).

The ability to design nanopores with bespoke structures, shapes and chemical properties will provide a well-defined environment for the precise control of single-molecule catalysis. By taking advantage of nanopores designed at the molecular scale, catalytic sites might be introduced into a protein nanopore lumen; then, reactant molecules captured inside the nanopore can be catalysed to form a product that is further released and translocated through the nanopore. This would provide a bottom-up approach for the production of customized chemicals. Presuming that a likely ultimate speed for the product formation is 1 ms per molecule, an array of 100 nanopores working in parallel would yield approximately  $3.6 \times 10^8$  products in less than 1 h. Nanopores have also been increasingly used as force transducers, allowing the controlled localization, trapping and orientation of a diverse range of biomolecules for single-molecule biophysics studies<sup>130,139</sup>. Finally, nanopore-based biomedical applications have developed beyond DNA sequencing and epigenetic modification analyses, and are now used to sense molecular biomarkers (proteins, metabolites and nucleic acids) in biofluids and other biological specimens. Given the fast growth rate of nanopore applications, it is likely that nanopore technology will become a prominent technique in single-molecule *in vitro* diagnostics.

In parallel with advances in nanopore design, portable nanopore devices consisting of millions of individual pores on a chip could produce enormous amounts of sensing data at high speeds. Similar devices could be used for the retrieval of various forms of data stored in DNA<sup>140,141</sup> or other polymers<sup>142</sup>.

Received: 26 November 2021; Accepted: 2 June 2022;  
Published online: 26 September 2022

## References

- Kasianowicz, J. J., Brandin, E., Branton, D. & Deamer, D. W. Characterization of individual polynucleotide molecules using a membrane channel. *Proc. Natl Acad. Sci. USA* **93**, 13770–13773 (1996).
- Kasianowicz, J., Walker, B., Krishnaswamy, M. & Bayley, H. Genetically engineered pores as metal ion biosensors. *MRS Proc.* **330**, 217–223 (1993).
- Bayley, H. & Cremer, P. S. Stochastic sensors inspired by biology. *Nature* **413**, 226–230 (2001).
- Li, J. et al. Ion-beam sculpting at nanometre length scales. *Nature* **412**, 166–169 (2001).
- Storm, A. J., Chen, J. H., Ling, X. S., Zandbergen, H. W. & Dekker, C. Fabrication of solid-state nanopores with single-nanometre precision. *Nat. Mater.* **2**, 537–540 (2003).
- Ying, Y.-L., Cao, C., Hu, Y.-X. & Long, Y.-T. A single biomolecule interface for advancing the sensitivity, selectivity, and accuracy of sensors. *Natl Sci. Rev.* **5**, 450–452 (2018).
- Clarke, J. et al. Continuous base identification for single-molecule nanopore DNA sequencing. *Nat. Nanotechnol.* **4**, 265–270 (2009).
- Cherf, G. M. et al. Automated forward and reverse ratcheting of DNA in a nanopore at 5-Å precision. *Nat. Biotechnol.* **30**, 344–348 (2012).
- Manrao, E. A. et al. Reading DNA at single-nucleotide resolution with a mutant MspA nanopore and phi29 DNA polymerase. *Nat. Biotechnol.* **30**, 349–353 (2012).
- Cao, C. et al. Discrimination of oligonucleotides of different lengths with a wild-type aerolysin nanopore. *Nat. Nanotechnol.* **11**, 713–718 (2016).
- Wanunu, M. et al. Rapid electronic detection of probe-specific microRNAs using thin nanopore sensors. *Nat. Nanotechnol.* **5**, 807–814 (2010).
- Sutherland, T. C. et al. Structure of peptides investigated by nanopore analysis. *Nano Lett.* **4**, 1273–1277 (2004).
- Movileanu, L., Schmittschmitt, J. P., Scholtz, J. M. & Bayley, H. Interactions of peptides with a protein pore. *Biophys. J.* **89**, 1030–1045 (2005).
- Movileanu, L., Howorka, S., Braha, O. & Bayley, H. Detecting protein analytes that modulate transmembrane movement of a polymer chain within a single protein pore. *Nat. Biotechnol.* **18**, 1091–1095 (2000).
- Nir, I., Huttner, D. & Meller, A. Direct sensing and discrimination among ubiquitin and ubiquitin chains using solid-state nanopores. *Biophys. J.* **108**, 2340–2349 (2015).
- Squires, A., Atas, E. & Meller, A. Nanopore sensing of individual transcription factors bound to DNA. *Sci. Rep.* **5**, 11643 (2015).
- Ketterer, P. et al. DNA origami scaffold for studying intrinsically disordered proteins of the nuclear pore complex. *Nat. Commun.* **9**, 902 (2018).
- Fisher, P. D. E. et al. A programmable DNA origami platform for organizing intrinsically disordered nucleoporins within nanopore confinement. *ACS Nano* **12**, 1508–1518 (2018).
- Gilboa, T., Zrehen, A., Girsault, A. & Meller, A. Optically-monitored nanopore fabrication using a focused laser beam. *Sci. Rep.* **8**, 9765 (2018).
- Yamazaki, H., Hu, R., Zhao, Q. & Wanunu, M. Photothermally assisted thinning of silicon nitride membranes for ultrathin asymmetric nanopores. *ACS Nano* **12**, 12472–12481 (2018).
- Kwok, H., Briggs, K. & Tabard-Cossa, V. Nanopore fabrication by controlled dielectric breakdown. *PLoS ONE* **9**, e28880 (2014).
- Waugh, M. et al. Solid-state nanopore fabrication by automated controlled breakdown. *Nat. Protoc.* **15**, 122–143 (2020).
- Xue, L. et al. Solid-state nanopore sensors. *Nat. Rev. Mater.* **5**, 931–951 (2020).
- Meller, A. Dynamics of polynucleotide transport through nanometre-scale pores. *J. Phys. Condens. Matter* **15**, R581–R607 (2003).
- Li, M.-Y. et al. Revisiting the origin of nanopore current blockage for volume difference sensing at the atomic level. *JACS Au* **1**, 967–976 (2021).
- Huo, M.-Z., Li, M.-Y., Ying, Y.-L. & Long, Y.-T. Is the volume exclusion model practicable for nanopore protein sequencing? *Anal. Chem.* **93**, 11364–11369 (2021).
- Mindell, J. A., Zhan, H., Huynh, P. D., Collier, R. J. & Finkelstein, A. Reaction of diphtheria toxin channels with sulfhydryl-specific reagents: observation of chemical reactions at the single molecule level. *Proc. Natl Acad. Sci. USA* **91**, 5272–5276 (1994).
- Walker, B., Kasianowicz, J., Krishnaswamy, M. & Bayley, H. A pore-forming protein with a metal-actuated switch. *Protein Eng. Des. Sel.* **7**, 655–662 (1994).
- Boersma, A. J. & Bayley, H. Continuous stochastic detection of amino acid enantiomers with a protein nanopore. *Angew. Chem. Int. Ed.* **51**, 9606–9609 (2012).
- Ouldali, H. et al. Electrical recognition of the twenty proteinogenic amino acids using an aerolysin nanopore. *Nat. Biotechnol.* **38**, 176–181 (2020).
- Li, M.-Y. et al. Unveiling the heterogeneous dephosphorylation of DNA using an aerolysin nanopore. *ACS Nano* **14**, 12571–12578 (2020).
- Wang, Y., Zheng, D., Tan, Q., Wang, M. X. & Gu, L.-Q. Nanopore-based detection of circulating microRNAs in lung cancer patients. *Nat. Nanotechnol.* **6**, 668–674 (2011).
- Galenkamp, N. S., Soskine, M., Hermans, J., Wloka, C. & Maglia, G. Direct electrical quantification of glucose and asparagine from bodily fluids using nanopores. *Nat. Commun.* **9**, 4085 (2018).
- Burck, N. et al. Nanopore identification of single nucleotide mutations in circulating tumor DNA by multiplexed ligation. *Clin. Chem.* **67**, 753–762 (2021).



35. Wang, Y. et al. Nanolock–nanopore facilitated digital diagnostics of cancer driver mutation in tumor tissue. *ACS Sens.* **2**, 975–981 (2017).
36. Jovanovic-Taliman, T. et al. Artificial nanopores that mimic the transport selectivity of the nuclear pore complex. *Nature* **457**, 1023–1027 (2009).
37. Kowalczyk, S. W. et al. Single-molecule transport across an individual biomimetic nuclear pore complex. *Nat. Nanotechnol.* **6**, 433–438 (2011).
38. Burns, J. R., Seifert, A., Fertig, N. & Howorka, S. A biomimetic DNA-based channel for the ligand-controlled transport of charged molecular cargo across a biological membrane. *Nat. Nanotechnol.* **11**, 152–156 (2016).
39. Fragasso, A. et al. A designer FG-Nup that reconstitutes the selective transport barrier of the nuclear pore complex. *Nat. Commun.* **12**, 2010 (2021).
40. Bayley, H., Luchian, T., Shin, S.-H. & Steffensen, M. in *Single Molecules and Nanotechnology* (eds Rigler, R. & Vogel, H.) 251–277 (Springer, 2008).
41. Liu, W., Yang, Z.-L., Yang, C.-N., Ying, Y.-L. & Long, Y.-T. Profiling single-molecule reaction kinetics under nanopore confinement. *Chem. Sci.* **13**, 4109–4114 (2022).
42. Talaga, D. S. & Li, J. Single-molecule protein unfolding in solid state nanopores. *J. Am. Chem. Soc.* **131**, 9287–9297 (2009).
43. Yusko, E. C. et al. Controlling protein translocation through nanopores with bio-inspired fluid walls. *Nat. Nanotechnol.* **6**, 253–260 (2011).
44. Oukhaled, G. et al. Unfolding of proteins and long transient conformations detected by single nanopore recording. *Phys. Rev. Lett.* **98**, 158101 (2007).
45. Soskine, M. et al. An engineered ClyA nanopore detects folded target proteins by selective external association and pore entry. *Nano Lett.* **12**, 4895–4900 (2012).
46. Huang, G. et al. Electro-osmotic vortices promote the capture of folded proteins by PlyAB nanopores. *Nano Lett.* **20**, 3819–3827 (2020).
47. Yusko, E. C. et al. Real-time shape approximation and fingerprinting of single proteins using a nanopore. *Nat. Nanotechnol.* **12**, 360–367 (2017).
48. Sha, J. et al. Identification of spherical and nonspherical proteins by a solid-state nanopore. *Anal. Chem.* **90**, 13826–13831 (2018).
49. Rotem, D., Jayasinghe, L., Salichou, M. & Bayley, H. Protein detection by nanopores equipped with aptamers. *J. Am. Chem. Soc.* **134**, 2781–2787 (2012).
50. Thakur, A. K. & Movileanu, L. Real-time measurement of protein–protein interactions at single-molecule resolution using a biological nanopore. *Nat. Biotechnol.* **37**, 96–101 (2019).
51. Wei, R., Gatterdam, V., Wieneke, R., Tampé, R. & Rant, U. Stochastic sensing of proteins with receptor-modified solid-state nanopores. *Nat. Nanotechnol.* **7**, 257–263 (2012).
52. Fahie, M. A., Yang, B., Mullis, M., Holden, M. A. & Chen, M. Selective detection of protein homologues in serum using an OmpG nanopore. *Anal. Chem.* **87**, 11143–11149 (2015).
53. Bell, N. A. W. & Keyser, U. F. Specific protein detection using designed DNA carriers and nanopores. *J. Am. Chem. Soc.* **137**, 2035–2041 (2015).
54. Bell, N. A. W. & Keyser, U. F. Digitally encoded DNA nanostructures for multiplexed, single-molecule protein sensing with nanopores. *Nat. Nanotechnol.* **11**, 645–651 (2016).
55. Mereuta, L. et al. Slowing down single-molecule trafficking through a protein nanopore reveals intermediates for peptide translocation. *Sci. Rep.* **4**, 3885 (2014).
56. Long, Y. & Zhang, M. Self-assembling bacterial pores as components of nanobiosensors for the detection of single peptide molecules. *Sci. China Ser. B* **52**, 731–733 (2009).
57. Rosen, C. B., Rodriguez-Larrea, D. & Bayley, H. Single-molecule site-specific detection of protein phosphorylation with a nanopore. *Nat. Biotechnol.* **32**, 179–181 (2014).
58. Robertson, J. W. F. et al. Single-molecule mass spectrometry in solution using a solitary nanopore. *Proc. Natl Acad. Sci. USA* **104**, 8207–8211 (2007).
59. Chavis, A. E. et al. Single molecule nanopore spectrometry for peptide detection. *ACS Sens.* **2**, 1319–1328 (2017).
60. Wang, H.-Y., Ying, Y.-L., Li, Y., Kraatz, H.-B. & Long, Y.-T. Nanopore analysis of  $\beta$ -amyloid peptide aggregation transition induced by small molecules. *Anal. Chem.* **83**, 1746–1752 (2011).
61. Huang, G., Willems, K., Soskine, M., Wloka, C. & Maglia, G. Electro-osmotic capture and ionic discrimination of peptide and protein biomarkers with FraC nanopores. *Nat. Commun.* **8**, 935 (2017).
62. Niu, H., Li, M.-Y., Ying, Y.-L. & Long, Y.-T. An engineered third electrostatic constriction of aerolysin to manipulate heterogeneously charged peptides transport. *Chem. Sci.* **13**, 2456–2461 (2022).
63. Zhang, S. et al. Bottom-up fabrication of a proteasome–nanopore that unravels and processes single proteins. *Nat. Chem.* **13**, 1192–1199 (2021).
64. Piguet, F. et al. Identification of single amino acid differences in uniformly charged homopolymeric peptides with aerolysin nanopore. *Nat. Commun.* **9**, 966 (2018).
65. Li, S., Cao, C., Yang, J. & Long, Y.-T. Detection of peptides with different charges and lengths by using the aerolysin nanopore. *ChemElectroChem* **6**, 126–129 (2019).
66. Restrepo-Pérez, L., Wong, C. H., Maglia, G., Dekker, C. & Joo, C. Label-free detection of post-translational modifications with a nanopore. *Nano Lett.* **19**, 7957–7964 (2019).
67. Nivala, J., Marks, D. B. & Akeson, M. Unfoldase-mediated protein translocation through an  $\alpha$ -hemolysin nanopore. *Nat. Biotechnol.* **31**, 247–250 (2013).
68. Nivala, J., Mulroney, L., Li, G., Schreiber, J. & Akeson, M. Discrimination among protein variants using an unfoldase-coupled nanopore. *ACS Nano* **8**, 12365–12375 (2014).
69. Brinkerhoff, H., Kang, A. S. W., Liu, J., Aksimentiev, A. & Dekker, C. Multiple rereads of single proteins at single-amino acid resolution using nanopores. *Science* **374**, 1509–1513 (2021).
70. Yan, S. et al. Single molecule ratcheting motion of peptides in a *Mycobacterium smegmatis* porin A (MspA) nanopore. *Nano Lett.* **21**, 6703–6710 (2021).
71. Chen, Z. et al. Controlled movement of ssDNA conjugated peptide through *Mycobacterium smegmatis* porin A (MspA) nanopore by a helicase motor for peptide sequencing application. *Chem. Sci.* **12**, 15750–15756 (2021).
72. Zhao, Q., de Zoysa, R. S. S., Wang, D., Jayawardhana, D. A. & Guan, X. Real-time monitoring of peptide cleavage using a nanopore probe. *J. Am. Chem. Soc.* **131**, 6324–6325 (2009).
73. Meng, F.-N., Ying, Y.-L., Yang, J. & Long, Y.-T. A wild-type nanopore sensor for protein kinase activity. *Anal. Chem.* **91**, 9910–9915 (2019).
74. Craig, J. M. et al. Revealing dynamics of helicase translocation on single-stranded DNA using high-resolution nanopore tweezers. *Proc. Natl Acad. Sci. USA* **114**, 11932–11937 (2017).
75. Ching-Wen, H. et al. Engineering a nanopore with co-chaperonin function. *Sci. Adv.* **1**, e1500905 (2021).
76. Cheley, S., Xie, H. & Bayley, H. A genetically encoded pore for the stochastic detection of a protein kinase. *ChemBioChem* **7**, 1923–1927 (2006).
77. Zernia, S., van der Heide, N. J., Galenkamp, N. S., Gouridis, G. & Maglia, G. Current blockades of proteins inside nanopores for real-time metabolome analysis. *ACS Nano* **14**, 2296–2307 (2020).
78. Wang, H. Y., Gu, Z., Cao, C., Wang, J. & Long, Y. T. Analysis of a single  $\alpha$ -synuclein fibrillation by the interaction with a protein nanopore. *Anal. Chem.* **85**, 8254–8261 (2013).
79. Soskine, M., Biesemans, A. & Maglia, G. Single-molecule analyte recognition with ClyA nanopores equipped with internal protein adaptors. *J. Am. Chem. Soc.* **137**, 5793–5797 (2015).
80. Galenkamp, N. S., Biesemans, A. & Maglia, G. Directional conformer exchange in dihydrofolate reductase revealed by single-molecule nanopore recordings. *Nat. Chem.* **12**, 481–488 (2020).
81. Galenkamp, N. S. & Maglia, G. Single-molecule sampling of dihydrofolate reductase shows kinetic pauses and an endosteric effect linked to catalysis. *ACS Catal.* **12**, 1228–1236 (2022).
82. Hu, R. et al. Differential enzyme flexibility probed using solid-state nanopores. *ACS Nano* **12**, 4494–4502 (2018).
83. Liu, S.-C., Ying, Y.-L., Li, W.-H., Wan, Y.-J. & Long, Y.-T. Snapshotting the transient conformations and tracing the multiple pathways of single peptide folding using a solid-state nanopore. *Chem. Sci.* **12**, 3282–3289 (2021).
84. Schmid, S., Stömmer, P., Dietz, H. & Dekker, C. Nanopore electro-osmotic trap for the label-free study of single proteins and their conformations. *Nat. Nanotechnol.* **16**, 1244–1250 (2021).
85. Steffensen, M. B., Rotem, D. & Bayley, H. Single-molecule analysis of chirality in a multicomponent reaction network. *Nat. Chem.* **6**, 603–607 (2014).
86. Ramsay, W. J. & Bayley, H. Single-molecule determination of the isomers of D-glucose and D-fructose that bind to boronic acids. *Angew. Chem. Int. Ed.* **57**, 2841–2845 (2018).
87. Lee, J. & Bayley, H. Semisynthetic protein nanoreactor for single-molecule chemistry. *Proc. Natl Acad. Sci. USA* **112**, 13768–13773 (2015).
88. Luchian, T., Shin, S.-H. & Bayley, H. Kinetics of a three-step reaction observed at the single-molecule level. *Angew. Chem. Int. Ed.* **42**, 1926–1929 (2003).
89. Pulcu, G. S. et al. Single-molecule kinetics of growth and degradation of cell-penetrating poly(disulfide)s. *J. Am. Chem. Soc.* **141**, 12444–12447 (2019).
90. Lu, S., Li, W.-W., Rotem, D., Mikhailova, E. & Bayley, H. A primary hydrogen–deuterium isotope effect observed at the single-molecule level. *Nat. Chem.* **2**, 921–928 (2010).
91. Ramsay, W. J., Bell, N. A. W., Qing, Y. & Bayley, H. Single-molecule observation of the intermediates in a catalytic cycle. *J. Am. Chem. Soc.* **140**, 17538–17546 (2018).
92. Kang, X., Gu, L.-Q., Cheley, S. & Bayley, H. Single protein pores containing molecular adapters at high temperatures. *Angew. Chem. Int. Ed.* **44**, 1495–1499 (2005).
93. Luchian, T., Shin, S.-H. & Bayley, H. Single-molecule covalent chemistry with spatially separated reactants. *Angew. Chem. Int. Ed.* **42**, 3766–3771 (2003).

94. Qing, Y., Pulcu, G. S., Bell, N. A. W. & Bayley, H. Bioorthogonal cycloadditions with sub-millisecond intermediates. *Angew. Chem. Int. Ed.* **57**, 1218–1221 (2018).
95. Gu, L.-Q., Cheley, S. & Bayley, H. Electroosmotic enhancement of the binding of a neutral molecule to a transmembrane pore. *Proc. Natl Acad. Sci. USA* **100**, 15498–15503 (2003).
96. Qing, Y., Tamagaki-Asahina, H., Ionescu, S. A., Liu, M. D. & Bayley, H. Catalytic site-selective substrate processing within a tubular nanoreactor. *Nat. Nanotechnol.* **14**, 1135–1142 (2019).
97. Astumian, R. D. Microscopic reversibility as the organizing principle of molecular machines. *Nat. Nanotechnol.* **7**, 684–688 (2012).
98. Qing, Y., Ionescu, S. A., Pulcu, G. S. & Bayley, H. Directional control of a processive molecular hopper. *Science* **361**, 908–912 (2018).
99. Qing, Y. & Bayley, H. Enzymeless DNA base identification by chemical stepping in a nanopore. *J. Am. Chem. Soc.* **143**, 18181–18187 (2021).
100. Hille, B. *Channels of Excitable Membranes* (Sinauer Associates, 2001).
101. Dekker, P. J. et al. Preprotein translocase of the outer mitochondrial membrane: molecular dissection and assembly of the general import pore complex. *Mol. Cell Biol.* **18**, 6515–6524 (1998).
102. Terry, L. J. & Wenthe, S. R. Flexible gates: dynamic topologies and functions for FG nucleoporins in nucleocytoplasmic transport. *Eukaryot. Cell* **8**, 1814–1827 (2009).
103. Driessen, A. J. M. & Nouwen, N. Protein translocation across the bacterial cytoplasmic membrane. *Annu. Rev. Biochem.* **77**, 643–667 (2008).
104. Baker, T. A. & Sauer, R. T. ClpXP, an ATP-powered unfolding and protein-degradation machine. *Biochim. Biophys. Acta Mol. Cell Res.* **1823**, 15–28 (2012).
105. Delcour, A. H. *Electrophysiology of Unconventional Channels and Pores* (Springer, 2015).
106. Sugawara, T. et al. Structural basis for pore-forming mechanism of staphylococcal  $\alpha$ -hemolysin. *Toxicon* **108**, 226–231 (2015).
107. Wang, S., Ji, Z., Yan, E., Haque, F. & Guo, P. Three-step channel conformational changes common to DNA packaging motors of bacterial viruses T3, T4, SPP1, and phi29. *Virology* **500**, 285–291 (2017).
108. Howorka, S. Building membrane nanopores. *Nat. Nanotechnol.* **12**, 619–630 (2017).
109. Siwy, Z. & Fuliński, A. Fabrication of a synthetic nanopore ion pump. *Phys. Rev. Lett.* **89**, 198103 (2002).
110. Hou, X. et al. A biomimetic potassium responsive nanochannel: G-quadruplex DNA conformational switching in a synthetic nanopore. *J. Am. Chem. Soc.* **131**, 7800–7805 (2009).
111. Xia, F. et al. Gating of single synthetic nanopores by proton-driven DNA molecular motors. *J. Am. Chem. Soc.* **130**, 8345–8350 (2008).
112. Ohmann, A. et al. A synthetic enzyme built from DNA flips 107 lipids per second in biological membranes. *Nat. Commun.* **9**, 2426 (2018).
113. Franceschini, L., Soskine, M., Biesemans, A. & Maglia, G. A nanopore machine promotes the vectorial transport of DNA across membranes. *Nat. Commun.* **4**, 2415 (2013).
114. Bayoumi, M., Nomidis, S. K., Willems, K., Carlon, E. & Maglia, G. Autonomous and active transport operated by an entropic DNA piston. *Nano Lett.* **21**, 762–768 (2021).
115. Spruijt, E., Tusk, S. E. & Bayley, H. DNA scaffolds support stable and uniform peptide nanopores. *Nat. Nanotechnol.* **13**, 739–745 (2018).
116. Kim, S. J. et al. Integrative structure and functional anatomy of a nuclear pore complex. *Nature* **555**, 475–482 (2018).
117. Jovanovic-Talisman, T. & Zilman, A. Protein transport by the nuclear pore complex: simple biophysics of a complex biomachine. *Biophys. J.* **113**, 6–14 (2017).
118. Ananth, A. N. et al. Spatial structure of disordered proteins dictates conductance and selectivity in nuclear pore complex mimics. *Elife* **7**, e31510 (2018).
119. Stanley, G. J. et al. Quantification of biomolecular dynamics inside real and synthetic nuclear pore complexes using time-resolved atomic force microscopy. *ACS Nano* **13**, 7949–7956 (2019).
120. Kelley, S. O. What are clinically relevant levels of cellular and biomolecular analytes? *ACS Sens.* **2**, 193–197 (2017).
121. Rozevsky, Y. et al. Quantification of mRNA expression using single-molecule nanopore sensing. *ACS Nano* **14**, 13964–13974 (2020).
122. Spitzberg, J. D., van Kooten, X. F., Bercovici, M. & Meller, A. Microfluidic device for coupling isotachophoretic sample focusing with nanopore single-molecule sensing. *Nanoscale* **12**, 17805–17811 (2020).
123. Freedman, K. J. et al. Nanopore sensing at ultra-low concentrations using single-molecule dielectrophoretic trapping. *Nat. Commun.* **7**, 10217 (2016).
124. Tian, K. et al. Single locked nucleic acid-enhanced nanopore genetic discrimination of pathogenic serotypes and cancer driver mutations. *ACS Nano* **12**, 4194–4205 (2018).
125. Zahid, O. K. et al. Solid-state nanopore analysis of human genomic DNA shows unaltered global 5-hydroxymethylcytosine content associated with early-stage breast cancer. *Nanomedicine* **35**, 102407 (2021).
126. Sze, J. Y. Y., Ivanov, A. P., Cass, A. E. G. & Edel, J. B. Single molecule multiplexed nanopore protein screening in human serum using aptamer modified DNA carriers. *Nat. Commun.* **8**, 1552 (2017).
127. Morin, T. J. et al. A handheld platform for target protein detection and quantification using disposable nanopore strips. *Sci. Rep.* **8**, 14834 (2018).
128. Cai, S., Sze, J. Y. Y., Ivanov, A. P. & Edel, J. B. Small molecule electro-optical binding assay using nanopores. *Nat. Commun.* **10**, 1797 (2019).
129. Thakur, A. K. & Movileanu, L. Single-molecule protein detection in a biofluid using a quantitative nanopore sensor. *ACS Sens.* **4**, 2320–2326 (2019).
130. Mathé, J., Visram, H., Viasnoff, V., Rabin, Y. & Meller, A. Nanopore unzipping of individual DNA hairpin molecules. *Biophys. J.* **87**, 3205–3212 (2004).
131. Lucas, F. L. R. et al. Automated electrical quantification of vitamin B1 in a bodily fluid using an engineered nanopore sensor. *Angew. Chem. Int. Ed.* **60**, 22849–22855 (2021).
132. He, L. et al. Digital immunoassay for biomarker concentration quantification using solid-state nanopores. *Nat. Commun.* **12**, 5348 (2021).
133. Rauf, S., Zhang, L., Ali, A., Liu, Y. & Li, J. Label-free nanopore biosensor for rapid and highly sensitive cocaine detection in complex biological fluids. *ACS Sens.* **2**, 227–234 (2017).
134. Rivas, F. et al. Label-free analysis of physiological hyaluronan size distribution with a solid-state nanopore sensor. *Nat. Commun.* **9**, 1037 (2018).
135. Vorobieva, A. A. et al. De novo design of transmembrane  $\beta$  barrels. *Science* **371**, eabc8182 (2021).
136. Shimizu, K. et al. De novo design of a nanopore for single-molecule detection that incorporates a  $\beta$ -hairpin peptide. *Nat. Nanotechnol.* **17**, 67–75 (2022).
137. Thomsen, R. P. et al. A large size-selective DNA nanopore with sensing applications. *Nat. Commun.* **10**, 5655 (2019).
138. Fragasso, A. et al. Reconstitution of ultrawide DNA origami pores in liposomes for transmembrane transport of macromolecules. *ACS Nano* **15**, 12768–12779 (2021).
139. Wang, J. J. et al. Identification of single amino acid chiral and positional isomers using an electrostatically asymmetric nanopore. *J. Am. Chem. Soc.* **144**, 15072–15078 (2022).
140. Chen, K., Zhu, J., Bošković, F. & Keyser, U. F. Nanopore-based DNA hard drives for rewritable and secure data storage. *Nano Lett.* **20**, 3754–3760 (2020).
141. Bell, N. A. W. & Keyser, U. F. Digitally encoded DNA nanostructures for multiplexed single-molecule protein sensing with nanopores. *Nat. Nanotechnol.* **11**, 645–651 (2016).
142. Dal Peraro, M. et al. Aerolysin nanopores decode digital information stored in tailored macromolecular analytes. *Sci. Adv.* **6**, eabc2661 (2020).

## Acknowledgements

Y.-T.L., Y.-L.Y. and Z.-L.H. acknowledge support from the National Natural Science Foundation of China (grant nos. 22027806, 21922405 and 22106066). G.M. acknowledges an ERC consolidator grant (no. 726151). A.M. acknowledges support from an ERC advanced grant (no. 833399). H.B. acknowledges an ERC advanced grant (no. 833792). Y.Q. acknowledges a Glasstone Research Fellowship and a Fellowship by Examination, Magdalen College, Oxford.

## Competing interests

The authors declare no competing interests.

## Additional information

**Correspondence** should be addressed to Giovanni Maglia, Amit Meller, Hagan Bayley, Cees Dekker or Yi-Tao Long.

**Reprints and permissions information** is available at [www.nature.com/reprints](http://www.nature.com/reprints).

**Publisher's note** Springer Nature remains neutral with regard to jurisdictional claims in published maps and institutional affiliations.

Springer Nature or its licensor holds exclusive rights to this article under a publishing agreement with the author(s) or other rightsholder(s); author self-archiving of the accepted manuscript version of this article is solely governed by the terms of such publishing agreement and applicable law.

© Springer Nature Limited 2022